ISBN: 978-3-95450-260-8 ISSN: 2673-5547 doi: 10.18429/JACoW-HIAT2025-FRA02

RARE-ISOTOPE PRODUCTION OPTICS OF ARIS PRESEPARATOR*

M. Portillo†, Y. Choi, S. Cogan, E. Daykin, A. Dombos, X. Du, K. Fukushima, M. Hausmann, D. Kahl, E. Kwan, S. Lidia, S. Miller, P. Nariyoshi, I. Nesterenko, F. Pereira, P. Ostroumov[1], X. Rao, B.M. Sherrill[1], M.K. Smith, J. Song, M. Steiner, O.B. Tarasov, T. Xu, T. Zhang,
Facility for Rare Isotope Beams, MSU, East Lansing, MI, USA
[1]also at the Department of Physics and Astronomy, MSU, East Lansing, MI, USA

Abstract

The Advance Rare Isotope Separator (ARIS) at FRIB provides in-flight purification of rare-isotope beams (RIB) generated by projectile fragmentation or fission on a target. Beams of stable ions from a driver linac impinge on a graphite target thin enough such that products maintain velocities close to that of the incident beam. The incident primary beam impinges on-target at about 200 MeV/u (for uranium and higher for lighter species). The energy may be lower than the maximum allowed, depending on the requirements of the experiment.

Using multi-charge state acceleration, the linac has most recently provided up to 20 kW on-target with a long-term goal of reaching 400 kW. Specialized magnets, collimators and other components have been integrated into the separator to withstand harsh conditions and facilitate maintenance. The optics properties at the beam dump are important since the power density must be kept low enough to avoid failure of the material. We describe the various optics modes that have been developed for safe operations and maximizing the beam power allowed for RIB production.

INTRODUCTION

The ARIS separator uses magnetic rigidity separation and momentum-loss achromat methods with wedged shaped degraders to purify beams of isotopes according to mass and atomic number *Z* [1].

The conceptual design was first introduced in a 2013 publication describing the optics and major components [2]. The layout addressed the major issues at the time, notably connecting the high-power driver linac (30 feet below ground level) to the existing experimental facility layout, while serving as a multi-stage in-flight separator. Figure 1 shows a schematic representation of the separator with labeled sections from target to diagnostic box DB5.

The description of each separation stage has already been described in detail by others [2, 3]. More details related to the separator role in operations at FRIB are also provided in these conference proceedings [4].

The focus here will be on the function of Stage 1 and the front-end optics solutions which have been developed for RIB operations. Details about beam transport after DB5 to experiments are described elsewhere [5].

* Work supported by the U.S. Department of Energy Office of Science under Cooperative Agreement DE-SC0023633, the State of Michigan, and Michigan State University.
† portillo@frib.msu.edu

Stage 1 Description

The first achromatic stage is often referred to as the vertical preseparator (PS). This stage is divided at wedge degrader position PSw, such that the front-end provides a momentum dispersion that is ~1/3 of that provided at the back-end, which ends at DB1. This is achieved by using 30º bend dipoles at the front-end and 50º at the back-end. A more detailed description of the magnets is provided in [6].

The latest optics solutions are very similar to the original design but have some slight differences due to slight changes during final construction. The first order matrix terms for the dispersion (x/d) and magnification (x/x) are listed in Table 1. The momentum compression factor can be determined to first order from the optics matrix terms using the following equation [7] :

$$\kappa = \frac{1}{(\mathrm{d/d})_{tot}} = -\frac{(x/\mathrm{d})_2}{(\mathrm{x/x})_2(\mathrm{x/d})_1} \quad (1)$$

Table 1: PS Optics Properties as Described in Text

Optics property	
$(x/d)_D$ Target to Dump [cm/%]	0.92
$(x/d)_1$ Target to PSw	-2.5
$(x/d)_2$ PSw to DB1	7.7
$(x/x)_2$	1.02
p-compression	3.0

The front-end components are exposed to the highest levels of beam loss and radiation from mainly target and beam dump. High power components of the beam are absorbed as much as possible in collimators and thermal shielding on magnets. Beam power after DB1 is typically well below a few watts.

Optics Modes

Three optics modes from target to PSw have been developed to maintain levels of power density to a minimum at beam dump while maximizing the power on-target. They are given names A, B, and C-optics and their first order properties are described by the plots in Fig. 2 and values listed in Table 2. The momentum resolving power is based on first order and a 1 mm beam spot at target.

ISBN: 978-3-95450-260-8 ISSN: 2673-5547 doi: 10.18429/JACoW-HIAT2025-FRA02

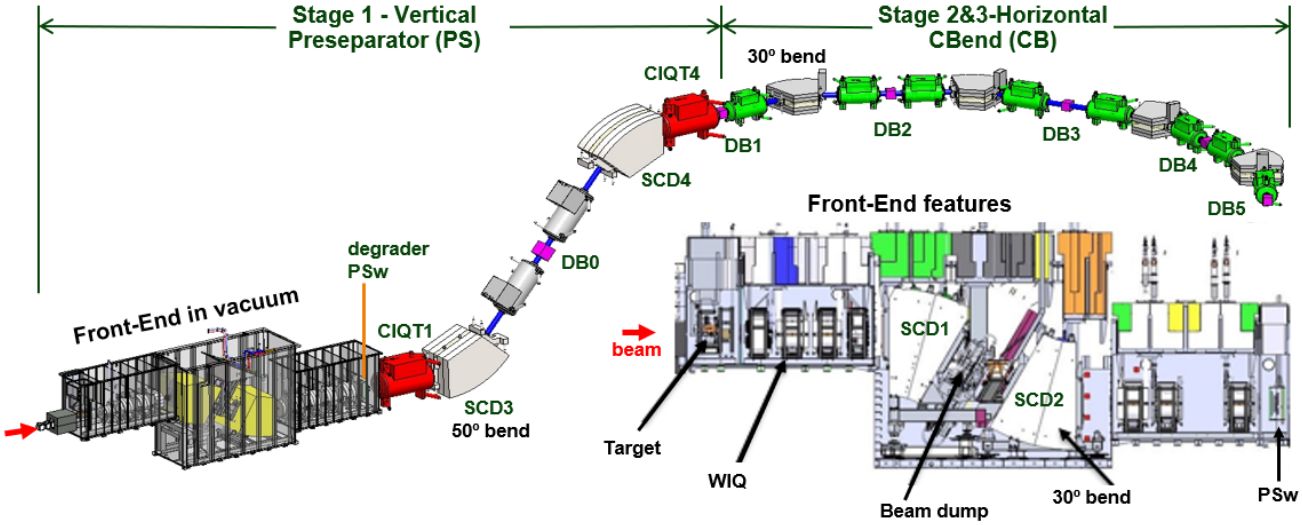

Figure 1: Layout of ARIS separator system from target to DB5. Three achromatic stages of separation purify the desired secondary beams to be delivered to experimental stations. The front-end magnets reside in vacuum and consist of WIQs. The rest of the quadrupoles are in cold-iron triplets (CIQT). See the text for more details.

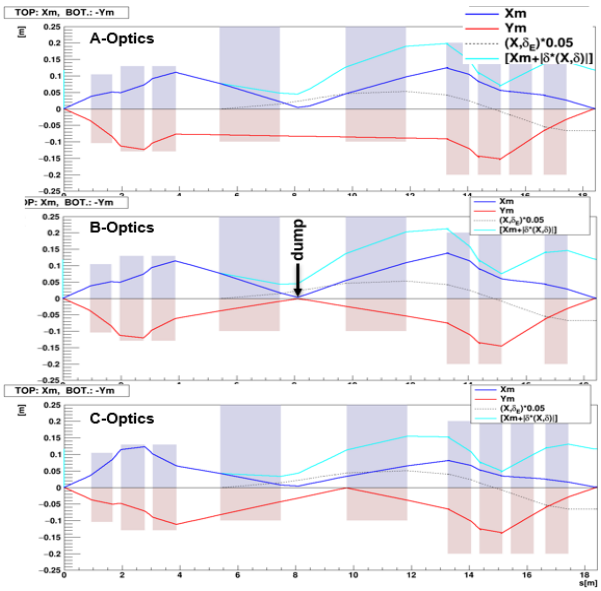

Figure 2: First order beam envelope plots of three solutions for PS target-to-wedge as described in the text.

Table 2: First Order Matrix Terms at PSw for Each Optics

Optics	(x/x)	(y/y)	*Rp* [mm]
A	1.50	-1.20	-1660
B	1.41	1.26	-1780
C	2.45	1.33	-1030

All three have the same dispersion of -2.5 cm/% and are used with the same back-end optics such that the compression factor remains the same to first order as evident by equation (1). As a result, the same wedge shape can be used to obtain achromatic focus at DB1.

All three modes have an x-focus at or close to the dump position. A-optics is closest to the original solution and is characterized by a parallel-y focus at dump position. B-optics is optimized to have y-focus at dump, while C-optics has polarities flipped in the first three warm-iron quadrupoles (WIQs) to reduce the chromatic aberrations in y.

The effects of higher order aberrations can be seen by the x versus y beam spot distributions at dump position as depicted in Fig. 3. (Red-dased lines depect the SCD1 dipole exit aperture boundaries.) The rays simulations were performed for 180 MeV/u ^{48}Ca primary beam. Only the 20+ charge state after an 8 mm graphite target was considered at various rigidity settings of the separator. The scale labeled dp/p at the top corresponds to the percentage difference from that centered on the optic axis. The simulations are carried out with fifth order maps evaluated using COSY INFINITY then imported into a LISE++ model as described elsewhere [8].

Notice that the beam widths in both x and y vary with dp/p setting such that small spot sizes result close to zero. High intensity RIB products tend to be close to the primary beam. When such products are selected it is necessary to choose the optics mode that will have size to minimize power density. Otherwise, the beam intensity needs to be limited to keep the estimated temperature on the beam dump below acceptable limits.

The expected beam widths for A-optics were confirmed with 1 kW operations using the so-called 20° beam dump, as described in [3]. This lends confidence to the simulation model. The larger incline of the currently used 6° beam dump allows for up to 20 kW operations, depending on the beam spot size [4].

The beam width behavior as a function of dp/p can be understood from the Taylor expansion terms of the map plotted in Fig. 4 as a function of the beam position up to PSw. Note that the A- and B-optics have a (y/bd) that swings wide and has a high slope for B-optics. This explains the large y-widths at the extremes. The C-optics has a reduced effect at the expense of a larger (x/ad) term which results in x-broadening of the beam at the extremes. Note that these simulations are for higher order correctors off.

ISBN: 978-3-95450-260-8 ISSN: 2673-5547 doi: 10.18429/JACoW-HIAT2025-FRA02

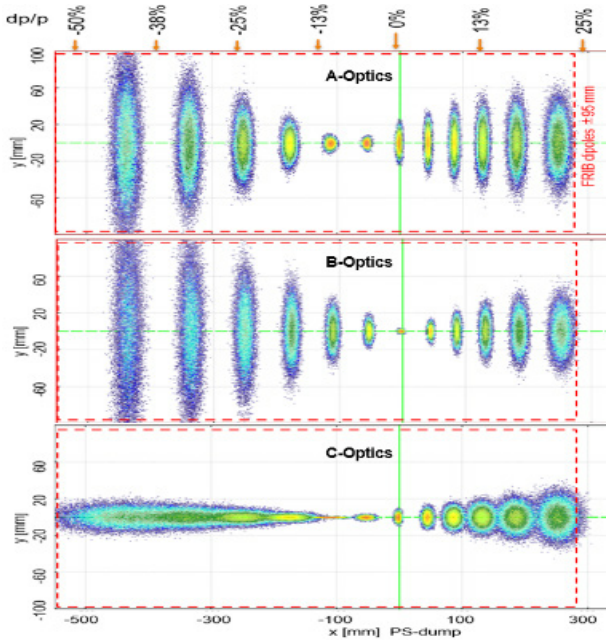

Figure 3: 5th order Monte Carlo simulation of rays from target to beam dump position as described in text.

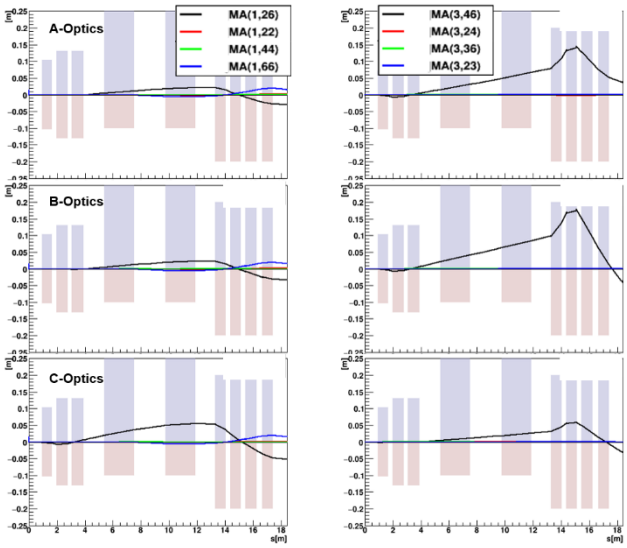

Figure 4: Plots of most prominent 2nd order map terms from target to PSw. (Left) x- and (Right) y-terms are such that terms x≡1, a≡2, y≡3, b≡4 and d=6.

Modes A and B have been used for routine operations over the past two years. The experience has been that A-optics tends to exhibit less purity when switching from B. Such effects have been most pronounced for cases of large phase space, such as fission products from ^{238}U. Transmission is very sensitive to quadrupole settings and reoptimizing may reduce the discrepancy. Further studies will be needed to confirm this.

The C-optics is a relatively new development and has not been tested yet since switching polarities at the first WIQ is not currently possible. A power supply switch is due to be installed during the Summer 2025 shut down which will allow the operation of this mode. This mode is expected to be needed below dp/p≈-40% where undesired losses due to large y-width occur. The trade-off is that the resolving power *Rp* can be ~70% less than that of the A and B modes. However, often such cases are for lower *Z* products for which high *Rp* is not required to obtain good purity anyway.

SUMMARY

Various optics modes for the ARIS separator front-end have been developed to support operational flexibility. All three optics modes developed have the same first order dispersion up to the preseparator wedge position, allowing the use of a common back-end optics that results in momentum compression factor of 3.

We have demonstrated that the higher order properties of each optics affects the primary beam spot size differently at the beam dump. The size varies depending on the beam deflection away from the optic axis and must be evaluated for each high-power beam setting before use. Temperature rise estimates are carried out to determine the maximum allowed power.

REFERENCES

[1] K.-H. Schmidt, E. Hanelt, H. Geissel, G. Münzenberg, and J. P. Dufour, "The momentum-loss achromat — A new method for the isotopical separation of relativistic heavy ions," *Nucl. Instrum. Methods Phys. Res., Sect. A*, vol. 260, no. 2–3, pp. 287–303, Oct. 1987. doi:10.1016/0168-9002(87)90092-1

[2] M. Hausmann *et al.*, "Design of the Advanced Rare Isotope Separator ARIS at FRIB," *Nucl. Instrum. Methods Phys. Res., Sect. B*, vol. 317, pp. 349–353, Dec. 2013. doi:10.1016/j.nimb.2013.06.042

[3] M. Portillo *et al.*, "Commissioning of the Advanced Rare Isotope Separator ARIS at FRIB," *Nucl. Instrum. Methods Phys. Res., Sect. B*, vol. 540, pp. 151–157, Jul. 2023. doi:10.1016/j.nimb.2023.04.025

[4] J. Wei *et al.*, "FRIB Operations: First three years", presented at HIAT'25, East Lansing, MI, Jun. 2025, paper MOX01, this conference.

[5] K. Fukushima *et al.*, "Rare isotope beam tuning in FRIB", presented at HIAT'25, East Lansing, MI, Jun. 2025, paper FRA01, this conference.

[6] Y. Choi *et al.*, "Overview of Fragment Separator Superconducting Magnets in the Facility for Rare Isotope Beams," *IEEE Trans. Appl. Supercond.*, vol. 33, no. 5, pp. 1–5, Aug. 2023. doi:10.1109/tasc.2023.3244141

[7] L. Bandura *et al.*, "Fragment separator momentum compression schemes," *Nucl. Instrum. Methods Phys. Res., Sect. A*, vol. 645, no. 1, pp. 182–186, Jul. 2011. doi:10.1016/j.nima.2010.12.015

[8] M. Portillo, M. Hausmann, and S. Chouhan, "Developments in magnet modeling and beam optics for the ARIS separator at FRIB," *Nucl. Instrum. Methods Phys. Res., Sect. B*, vol. 376, pp. 150–155, Jun. 2016. doi:10.1016/j.nimb.2016.01.029